International Journal of Scientific Research and Engineering Development-– Volume 8 Issue 4, July - Aug 2025

Available at www.ijsred.com

RESEARCH ARTICLE OPEN ACCESS

PERFORMANCE ANALYSIS of RECONFIGURABLE INTELLIGENT SURFACE (RIS) ASSISTED RADIO OVER FREE SPACE OPTICALCOMMUNICATION(ROFSO) SYSTEM OVER MALAGA FOR SMART CITY APPLICATIONS

Juwawa Chayangira*

*(Electronic Engineering Department, Harare Institute of Technology, Zimbabwe, Harare

Email: h231031h@hit.ac.zw)

--************************----------------------------------

Abstract:

The growing demand for high-capacity, low-latency, and energy-efficient communication infrastructure in smart cities has accelerated the exploration of hybrid technologies that integrate radio frequency (RF) and optical domains. **Reconfigurable Intelligent Surfaces (RIS)** have emerged as a transformative technology capable of dynamically shaping the wireless propagation environment, offering significant improvements in coverage, reliability, and energy efficiency. This paper investigates the performance of **RIS-assisted Radio-over-Free-Space Optical (RoFSO)** communication systems under **Málaga-M atmospheric turbulence fading**, a comprehensive statistical model well-suited for characterizing urban free-space optical channels. By leveraging RIS to intelligently reflect and redirect optical beams, the system can mitigate challenges such as non-line-of-sight (NLOS) propagation, atmospheric scattering, and beam misalignment caused by urban dynamics. Analytical expressions for key performance metrics, including **Average Bit Error Rate (ABER)** and **outage** probability, are derived using to capture the composite impact of fading, RIS configuration, and QAM modulation scheme. Simulation results validate the theoretical analysis and demonstrate that RIS deployment significantly enhances link robustness, even under severe turbulence and complex urban geometries. The proposed RIS-assisted RoFSO framework offers a promising pathway toward the realization of scalable, adaptive, and high-performance communication networks in future smart city environments.

Keywords — **Malaga, reconfigurable surfaces, are separated by comma.**

--************************----------------------------------

I. Introduction

Optical communication systems utilize either free space or optical fibres to transmit information bearing signals. These systems have become indispensable in the telecommunications sector due to their capability to support high-speed data transmission over long distances [1]. The core components include optical transmitters typically laser diodes or light-emitting diodes (LEDs)which convert electrical signals into optical signals. This process is illustrated schematically in Fig. 1 .

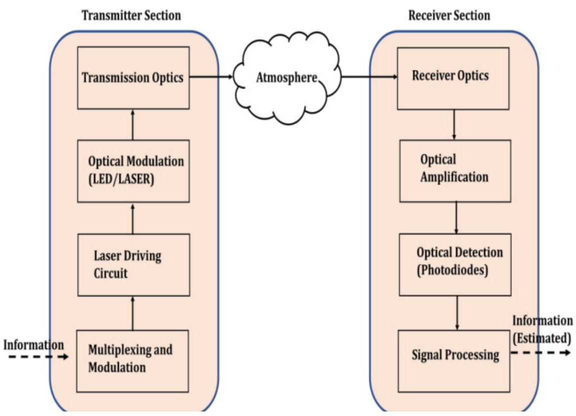

Fig. 1 Block diagram of the RoFSO system.

Fig. 1 shows the RoFSO basic block diagram. In RoFSO, the message or information signal is modulated onto an optical carrier and sent to the receiver through the atmosphere. The received optical signal is transformed back into an electrical signal and the information or message is estimated. Several statistical models have been proposed to describe atmospheric turbulence effects which include log normal, Gamma gamma and Malaga M. Compared with LN distribution, GG distribution can be used for all the turbulence regimes. In [2], the outage probability for multi-hop FSO system with DF protocol has been analysed based on the LN distribution. The FSO signal transmission via K-distributed atmospheric turbulence channel, when selection combining (SC), equal gain combining (EGC) or maximum ratio combining (MRC) is employed, was analysed in [13]. The analysis of the FSO system influenced by weak log-normal atmospheric turbulence conditions, employing SC and switch and-stay combining (SSC)/switch-and-examine (SEC) combining, was presented in [3] and [4], respectively. The Gamma-Gamma distribution is widely adopted for moderate to strong turbulence. It models both small- and large-scale eddies using two independent Gamma distributions, offering better accuracy across a wide range of conditions [5]. Gamma-Gamma PDF was suggested by Andrews et. al. as a reasonable choice because of its much more tractable mathematical model [6]. The outage probability and the average symbol error rate (ASER) of the multi-hop DF FSO links over the GG turbulence channels considering the path loss and pointing errors have been studied systematically in [7]. The BER performance of a serial relayed Ro-FSO OFDM system over Gamma-Gamma distribution is studied in [8].In a recent work[9, 10] the BER performance of Ro-FSO system based on OFDM scheme with QAM is analysed . In [11], the authors proposed an analysis considering an FSO system over a Gamma-Gamma channel model with distance and jitter ratios, while in[11] , the FSO channel is analysed in light of the Huygens principle for a transmission over the Gamma-Gamma channel for single and multiple FSO links, respectively. In [20], the authors proposed a multi-branch RIS assisted FSO system with multiple optical RIS infrastructures, based on the Gamma function. Assuming Gamma–Gamma atmospheric turbulence conditions, implementation of the spatial diversity techniques was observed in [12], while the effect of the pointing errors was added in [13].

In RoFSO, as the optical signal passes through the atmosphere, it is affected by atmospheric turbulence, pointing errors, and attenuation. In addition to these effects, the blocking of signals due to the presence of a mountain, building, or big tree can prevent the transmitted signal from arriving at the destination, which is called a skip zone or dead zone problem. A reconfigurable intelligent surface (RIS) is one of the solutions proposed to avoid the skip zone problem [14, 15]. An earlier RIS was utilized to solve the dead zone problem in wireless communications and initiate smart communication [16-18]. Because of an obstruction (such as a tall structure or tree), there is no line of sight between the source and the destination. It is believed that the RIS element's reflection allows a single light beam to travel from its source to its destination. Positioned on the top floor of a building, the RIS acts as a reflector for the incoming optical signal, directing the transmitted signal in the direction of the receiver. .RIS has emerged as a feasible option to reduce the skip or dead zone problem and enhance the signal-to-noise ratio (SNR) in wireless communication systems[19, 20] . In addition to fixing the skip zone problem, it provides channel reconfigurability to wireless systems [20, 21]. Fig. 2 shows the RIS-assisted RoFSO system.

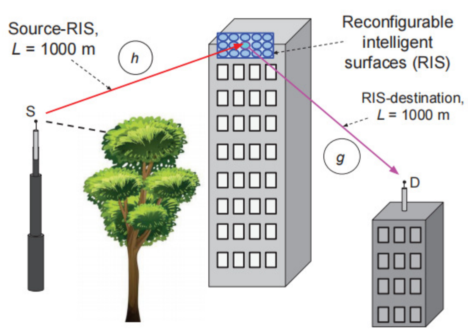

Fig. 2 Shows the RIS-assisted RoFSO system.

Unlike traditional technologies that rely on active relaying or complex antenna arrays, RIS is passive, low-power, and cost-effective, making it highly suitable for integration into the infrastructure **of** smart cities**,** indoor networks, and Internet of Things (IoT) ecosystems**.** The ability to control the wireless environment in real-time opens new opportunities for channel hardening**,** beamforming**,** and environment-aware network design**.**

RIS-enabled systems can transform objects like walls, building facades, or indoor panels into smart surfaces that reflect or refract signals toward intended receivers. This capability allows line-of-sight (LoS) restoration in blocked environments and supports robust communication links in scenarios affected by severe fading**,** mobility**, or** non-stationarity of users.

In the context of Free Space Optical (FSO) and Radio over FSO (RoFSO) communications, RIS can serve as a powerful tool to overcome challenges posed by atmospheric turbulence**,** pointing errors**,** and scattering**,** especially in urban environments characterized by dynamic and unpredictable channel conditions. The integration of RIS with FSO links, particularly over Málaga-M fading channels, is gaining significant research interest as a viable enabler for **B5G/6G** smart city applications. To the best of the author knowledge RIS-aided RoFSO over Malaga distribution was not fully investigated.The contributions from the research are as follows:

- RIS-aided RoFSO system over M-distributed turbulence with M-QAM modulation for smart city applications is proposed.
- The novel closed-form expressions of the probability density function (PDF), cumulative distribution function (CDF), outage probability (OP) and average bit error rate (ABER) for the proposed system are derived.
- OP is evaluated for different turbulence scenarios.
- The ABER performance of the proposed system under different turbulence regimes, link lengths, and scattering errors is investigated

SYSTEM and CHANNEL MODEL

We assume an ris-aided rofso communication system which consists of an optical source, an optical ris, and a destination, as shown in Fig. 2. due to the obstruction of buildings, there is no line of sight between the source and destination, with the communication being performed only through the ris, which is placed on top of a building to provide propagation of signal between source and destination. The received signal at the destination is given by

$$\boldsymbol{y = hx + n} \qquad \textbf{(1)}$$

Where y is the received signal that has been affected by atmospheric turbulence, x is the transmitted optical signal and $\mathbf{h} \in \mathbf{R}^{+}$ is the channel gain and n is the additive white Gaussian noise (AWGN). The signal suffer from atmospheric turbulence, pointing errors as it passes through the free space channel (FSO)

A. *System Model*

From Fig.2 the RIS-assisted RoFSO system there is an obstruction (such as a tall structure or tree), there is no line of sight between the source and the destination. It is assumed that the RIS element's reflection allows a single light beam to travel from its source to its destination. The RIS placed on the top floor of a building, reflects the incoming optical signal, directing the transmitted signal to the receiver.

Considering h and g which are complex channel vectors for the source to RIS path and RIS to detector path, respectively, it is assumed that the same atmospheric channel conditions exist for both sub channels, i.e., from transmitter to RIS and from RIS to receiver. Additionally, the pointing error at each receiving site is considered to be the same. Smart cities may easily implement the Malaga M model.

B. *FSO Channel model*

There are three major deterioration factors in the RoFSO link: attenuation, atmospheric turbulence, and pointing error. *:* In this study optical channel model I is considered as product of Ia , $I p$, and I_l which is given below [22]

$$I = Ia\, I_l\, I p \qquad (2)$$

where Ia , $I p$, and I_l represent the signal at the receiver that has been affected by atmospheric turbulence, pointing error, and attenuation, respectively

The M distribution is taken into consideration while modeling atmospheric turbulence. The M distribution is unique in that it can characterize almost all of the existing models of atmospheric turbulence, such as the gamma, gamma gamma, negative exponential, K distribution, and log normal models, and it covers all channel conditions from weak to strong turbulence. A) the line of sight [LOS] component with power Ω, B) the scattered component coupled to the line of sight component with power 2ρb0, and C) the scattered component independent of the other components with power 2(1 − ρ)b0[23] are the three components of the optical beam that are taken into consideration in the diagram below. Thus, 2b0 is the total power of the scattered components. where the coupling between the scattered components of the transmitted optical signal and the LOS is denoted by ρ.

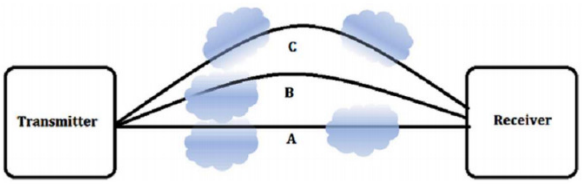

Fig. 3: FSO system beam propagation in Malaga model including small scale fluctuations [18]

The probability density function (PDF) of the Malaga-distribution turbulence is given by [24]

$$f_{Ia}(I_a) = A\sum_{m=1}^{\beta} a_m\, I_a^{\frac{\alpha+m}{2}-1} K_{\alpha-m}\left(2\sqrt{\frac{\alpha\beta I_a}{g\beta+\Omega}}\right) \quad (3)$$

where $$A = \frac{2\alpha^{\frac{\alpha}{2}}}{g^{1+\frac{\alpha}{2}}\Gamma(\alpha)}\left(\frac{g\beta}{g\beta+\Omega'}\right)^{\beta+\frac{\alpha}{2}} \quad (4)$$

$$a_m = \binom{\beta-1}{m-1}\frac{(g\beta+\Omega')^{1-\frac{m}{2}}}{m-1!}\left(\frac{\Omega'}{g}\right)^{m-1}\left(\frac{\alpha}{\beta}\right)^{\frac{m}{2}} \quad (5)$$

A is the effective number of large-scale cells during the scattering process. β is the natural number which makes the PDF to follow the observed data, leading to a closed-form equation [25]. Average power received by coherent contributions is given by

$\Omega' = \Omega + 2\rho b_0 + 2\sqrt{2b_0\rho}\,\cos(\phi_A - \phi_B)$, ϕ_A, ris the phase of the LOS component, and ϕ_B is the phase of the coupled-to-LOS component. The difference between ϕ_A and ϕ_B is taken to be 90˚.

A. *Pointing errors*

As seen in the Fig.4 below, building sways caused by pointing error effects at the receiver from wind movement and thermal heating cause a misalignment between the transmitter and receiver.

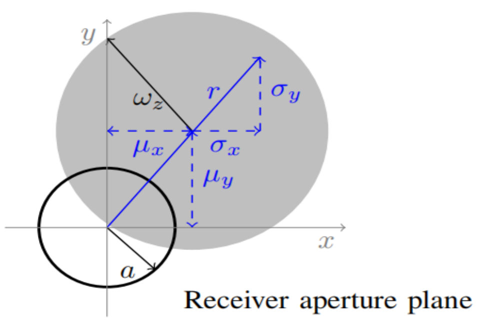

.

Fig. 4: Showing the effects pointing errors on the receiver.

The PDF for the pointing error as given by[26]

$$fIp\,(I_P) = \frac{\xi^2}{A_0^{\xi^2}}(I\,p)^{\xi^2}, \text{ for } 0 \le I\,p \le A_0, \quad (6)$$

Where ξ represents the ratio of the equivalent beam radius at the receiver to the jitter standard deviation.

$Ao = [\mathrm{erf}(v)]^2$, where erf(·) is error function, and $v = \frac{r\sqrt{\pi}}{\sqrt{2}w_z}$. r and w_z represent the radii of the receiver aperture and the beam waist, respectively. Finally, path loss , which can be considered as constant for a specific weather condition and distance [26], is modelled using the Beer–Lambert law and is given by $I_l = e^{-\delta L}$, where δ represents the attenuation factor, and L is the link length.

II. Combined Channel Model

The resultant channel model for I is given as [27]

$$f_{I/Ia}(I/Ia) = \int f_{I/Ia}(I/Ia)\, f_{Ia}(Ia)\,\mathrm{d}Ia. \quad (7)$$

Here, $fI/Ia\,(I/Ia)$ denotes the conditional probability, for a given turbulence state Ia . It is defined as [23]

$$f\,I/Ia\;(I/Ia) = \frac{1}{I_a I_l}\, fI_{\mathrm{p}}\left(\frac{I}{I_a I_l}\right)$$

$$= \frac{g^2}{A_0^{g^2}\, I a I_l}\left(\frac{I}{Ia\,Il}\right)^{g^2-1} \quad (8)$$

III. Closed-Form Statistical Analysis

In this section, closed-form expressions of the end-to-end PDF and CDF were derived.

A. End-to-End SNR

Only the optical signal reflected off the RIS surface is regarded as having been transferred from the source to the RIS. In addition, it is assumed that the channel phases at the RIS and desstination are known . The signal that the detector receives may be written as

$y = \sqrt{E_s}(h\mu e^{j\theta} g)x + n$ [1], where E_s represents the symbol energy, and h and g are complex channel vectors of the source to the RIS and RIS to the destination, respectively. μ and θ are parameters of the RIS element; μ *is* the amplitude reflection coefficient, and θ is the phase induced by the RIS module [18, 28]. x and y are the transmitted and received symbols, respectively. n is AWGN. The main goal of the RIS is to reflect the signal in the direction of the destination in order to maximize the signal-to-noise ratio (SNR) at that location. Maximization of the end-to-end SNR makes this feasible.

This maximized SNR is defined as $\gamma = \bar{\gamma}\left|h\mu e^{j\theta}\right|^2$

B. *PDF of End-to-End SNR*

The system gain is expresses as by $h\mu e^{j\theta}g$, where $\mu e^{j\theta}$ is deterministic, and h and g are random variables. Heterodyne Detection was considered in this study. Thus, the SNR's PDF $f_\gamma(\gamma)$is expressed as [29]

$$f_\gamma(\gamma) = \int_0^\infty f_{\gamma_h}(t)\, f_{\gamma_g}\left(\frac{\gamma}{t}\right)\frac{1}{t}\,dt. \tag{9}$$

Where γ_h and γ_g are the SNRs of the sub channels' source to RIS and RIS to the destination, respectively, and $f_{\gamma_g}(.)$ and f_{γ_h} are the PDFs of the respective sub channels. We have considered constant weather conditions, so both sub-channels

can be modelled with the same turbulence levels and pointing errors; this will result in a unified PDF defined as [26]

$$f_{\gamma_i}(\gamma_i) = \frac{\xi^2 A}{2\gamma_i}\sum_{m=1}^{\beta} b_m G_{1,3}^{3,0}\left[B\left(\frac{\gamma_i}{\bar{\gamma}_i}\right)\middle|\begin{matrix}\xi^2+1\\ \xi^2,\alpha,m\end{matrix}\right]. \tag{10}$$

Substituting successively γ_i with t and $\frac{\gamma}{t}$ into Eq. (10) and we get $f_{\gamma_h}(t)$ and $f_{\gamma_g}\left(\frac{\gamma}{t}\right)$ as

$$f_{\gamma_h}(t) = \frac{\xi^2 A}{2t}\sum_{m=1}^{\beta} b_m G_{1,3}^{3,0}\left[B\left(\frac{t}{\bar{\gamma}_h}\right)\middle|\begin{matrix}\xi^2+1\\ \xi^2,\alpha,m\end{matrix}\right]. \tag{11}$$

and

$$f_{\gamma_g}\left(\frac{\gamma}{t}\right) = \frac{\xi^2 At}{2\gamma}\sum_{m=1}^{\beta} b_m G_{1,3}^{3,0}\left[B\left(\frac{\gamma}{t\bar{\gamma}_g}\right)\middle|\begin{matrix}\xi^2+1\\ \xi^2,\alpha,m\end{matrix}\right]. \tag{12}$$

where $\bar{\gamma}_h$ and $\bar{\gamma}_g$ are the averages of SNRs γ_h and γ_g γg , respectively. The reflection property of the Meijer-G function is given by[30]

$$G_{p,q}^{m,n}\left[z\middle|\begin{matrix}A_p\\ B_q\end{matrix}\right] = G_{p,q}^{m,n}\left[z^{-1}\middle|\begin{matrix}1-B_q\\ 1-A_p\end{matrix}\right]. \tag{13}$$

Using the reflection property of the Meijer-G function, as given by Eq. (13), Eq. (12) is expressed as

$$f_{v_g}\left(\frac{\gamma}{t}\right) = \frac{\xi^2 At}{2\gamma}\sum_{m=1}^{\beta} b_m G_{3,1}^{0,3}\left[\left(\frac{t\bar{\gamma}_g}{\gamma}\right)\middle|\begin{matrix}1-\xi^2,1-\alpha,1-m\\ -\xi^2\end{matrix}\right]. \tag{14}$$

Substituting $f_{\gamma_h}(t)$ and $f_{\gamma_g}\left(\frac{\gamma}{t}\right)$ from Eqs. (11) and (14) into Eq. (9), and after solving [with help of [31], Eq. (13)], the end to-end PDF is given as

$$f_\gamma(\gamma) = \frac{\xi^2 A}{2}\sum_{m=1}^{\beta} b_m \frac{\xi^2 A}{2\gamma}\sum_{m=1}^{\beta} b_m \times G_{6,2}^{0,6}\left[\left(\frac{\bar{\gamma}}{B^2\gamma}\right)\middle|\begin{matrix}1-\xi^2,1-\alpha,1-m,1-\xi^2,1-\alpha,1-m\\ -\xi^2,-\xi^2\end{matrix}\right]. \tag{15}$$

Here $\bar{\gamma} = \bar{\gamma}_h\bar{\gamma}_g$ Applying the identity from Eq. (13), we get the PDF of the end-to-end SNR as

$$f_\gamma(\gamma) = \frac{\xi^2 A}{2}\sum_{m=1}^{\beta} b_m \frac{\xi^2 A}{2\gamma}\sum_{m=1}^{\beta} b_m G_{6,2}^{0,6}\left[\left(\left(\frac{B^2\gamma}{\bar{\gamma}_g}\right)\right)\middle|\begin{matrix}1+\xi^2,1+\xi^2\\ \xi^2,\alpha,m,\xi^2,\alpha,m\end{matrix}\right]. \tag{16}$$

C. *CDF of End-to-End SNR*

The CDF of the end-to-end SNR $F_\gamma(\gamma)$ is obtained from

$$F_\Upsilon(\gamma) = \int_0^\infty f_\gamma(\gamma)\, d\gamma \tag{17}$$

After substitution of $f_\gamma(\gamma)$ from Eq. (16) into Eq. (17) and substituting variables γ , x , and∞, we arrive at

$$F_\Upsilon(\gamma) = \frac{\xi^2 A}{2}\sum_{m=1}^{\beta} b_m \frac{\xi^2 A}{2}\sum_{m=1}^{\beta} b_m \times$$

0γ1xG2,66,0,B2xγg1+ξ2,1+ξ2ξ2,α,m,ξ2,α,mdx.
(18)

After solving Eq. (18) [with help of [23][, Eq. (07.34.21. 0084.01)], the CDF is expressed as

$$F_\Upsilon(\gamma) = \frac{\xi^2 A}{2}\sum_{m=1}^{\beta} b_m \frac{\xi^2 A}{2}\sum_{m=1}^{\beta} b_m \times$$

G3,76,1,bmB2γγ1, 1+ξ2,1+ξ2ξ2,α,m,ξ2,α,m0.
(19)

V. Performance Analysis

Based on the OP, ECC, and ABER for certain binary and M-QAM modulation schemes, the performance of the RIS assisted FSO system is examined.

A. *Outage Probability*

OP evaluates the FSO system's dependability. An outage occur when the end-to-end SNR drops below a certain threshold value for a particular quality of service. OP is defined as

$$\mathbf{P}_{out} = \mathbf{P}_r(\gamma \leq= \gamma_{th}) = F_\gamma(\gamma_{th}) \tag{20}$$

Thus, the OP, *P*out, of the RIS-assisted FSO system is given by evaluating $F_\gamma(\gamma_{th})$ from Eq. (20):

$$\mathbf{P}_{out} = \frac{\xi^2 A}{2}\sum_{m=1}^{\beta} b_m \frac{\xi^2 A}{2}\sum_{m=1}^{\beta} b_m \times$$
***G3,76,1,B2γthγ1,1+ξ2,1+ξ2ξ2,α,m,ξ2,α,m,*0.**
(21)

where γ_{th} is the threshold SNR.

B. *Average BER for M-QAM*

BER is an important metric used to evaluate system performance in FSO data transfer.
M-QAM modulation is investigated for the RIS-assisted FSO system. The ABER for M-QAM modulation is given by [32]

$$\overline{\mathrm{P}}_b = \frac{1-\frac{1}{\sqrt{M}}}{log_2 M}\int_0^\infty erfc\left(\sqrt{\frac{3log_2 M\gamma}{4(M-1)}}\right) f_\gamma(\gamma)d\gamma. \tag{22}$$

where, erfc(·) represents complementary error function. Using the complementary error function equivalent of the Meijer-G function [23], Eq. (06.27.26.0006.01), ABER for the considered M-QAM modulation scheme is evaluated as

$$\overline{\mathrm{P}}_b = \frac{1-\frac{1}{\sqrt{M}}}{log_2 M}\int_0^\infty G_{1,2}^{2,0}\left[\left(\frac{3log_2 M\gamma}{4(M-1)}\right)\middle|\begin{matrix}1\\0,\frac{1}{2}\end{matrix}\right]\times \frac{\xi^2 A}{2}\sum_{m=1}^{\beta} b_m \frac{\xi^2 A}{2\gamma}\sum_{m=1}^{\beta} b_m \times G_{2,6}^{6,,0}\left[\left(\frac{B^2\gamma}{\overline{\gamma}}\right)\middle|\begin{matrix}1+\xi^2, 1+\xi^2\\ \xi^2,\alpha,m,\xi^2,\alpha,m\end{matrix}\right]. \tag{23}$$

After solving Eq. (23) [with help of [31], Eq. (22)], we get the closed-form expression of ABER forM-QAM as

$$\overline{\mathrm{P}}_b = \frac{1-\frac{1}{\sqrt{M}}}{log_2 M\sqrt{\pi}}\frac{\xi^2 A}{2}\sum_{m=1}^{\beta} b_m \frac{\xi^2 A}{2}\sum_{m=1}^{\beta} b_m \times G_{4,7}^{6,2}\left[\left(\frac{4B^2(M-1)}{\overline{\gamma}3log_2 M}\right)\middle|\begin{matrix}1+\xi^2, 1+\xi^2, 1,0\\ \xi^2,\alpha,m,\xi^2,\alpha,m,\end{matrix}\right. \tag{24}$$

Table 1. System Variables for Numerical Findings [1]

RIS element diameter		1 [mm]	D
Jitter standard deviation		0,1 [cm]	(σs)
Wavelength		1550 [nm]	λ
Beam waist at transmitter		4 [cm]	ω_0
Receiver aperture diameter		1 [mm]	*d*

VI. Numerical Results and Discussions

In this study, the RIS-aided RoFSO system was investigated. The source and destination are located at the same distance, L km, from the RIS and 1550 nm optical wavelength is considered . Both subchannels of the system are characterized by the same refractive structure and index, c_n^2, which remains constant during one-symbol transmission. $c_n^2 = (5 \times$ *10−13m−23 , cn2=2.5×10−13m−23*, and $c_n^2 = (10 \times 10^{-14})m^{-\frac{2}{3}}$are considered for strong, moderate, and weak turbulence, respectively. In the proposed RIS-assisted FSO system, the elements of the RIS and receiver aperture are considered to have the same diameter: *D* = 1mm .

Fig.5 shows the OP with the threshold SNR taken as 9 dB in different turbulence conditions.

The link length is taken as 1 km, and the scattering parameter ρ is 0.596. It can be observed in Fig. 3 that as the turbulence strength increases, the OP also increases, which means system performance is affected by atmospheric turbulence. To maintain the 10–2 OP, the system requires almost 27 dB SNR in a weak turbulence condition, 37dB SNR in a moderate turbulence condition, and 43 dB SNR in a strong turbulence condition.

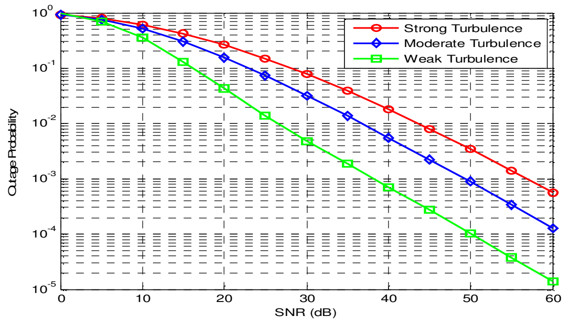

Fig. 5 OP results showing the performance of the RIS-assisted RoFSO system with different turbulence conditions in terms of the SNR (link length 1 km, scattering parameter $\rho = 0.596$).

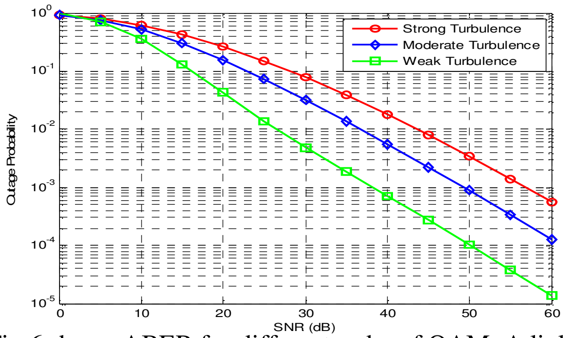

Fig.6 shows ABER for different order of QAM. A link length of 1 km and moderate condition was considered.

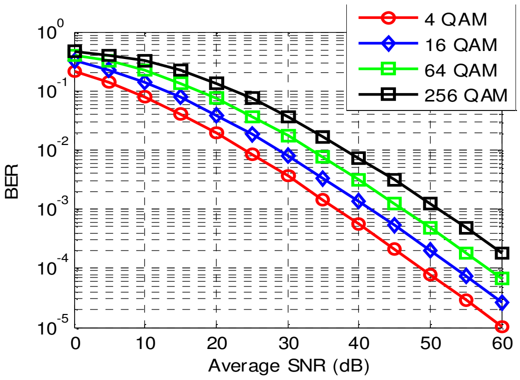

Fig. 6 ABER against SNR with various QAM and moderate turbulence in the proposed RIS-assisted RoFSO system (moderate atmospheric turbulence, link length 1 km, scattering parameter ρ = 0.596)

It is clear from the Fig.6 that as we increase the order of QAM, the data transmitted through the link increase, which means that the spectral efficiency increases as BER also increases. There is a trade-off between reliability and effectiveness in communication. When very high spectral efficiency is not required, 16-QAM is better than higher-QAM formats. Thus, in this study, 16-QAM modulation is considered. From the graph, it can be observed that to maintain 10^{-3} ABER, 4-QAM requires 38 dB SNR, 16-QAM requires 41 dB SNR, 64-QAM requires 47 dB SNR, and 256 QAM requires more than 50 dB SNR.

Conclusion

The performance of the RIS-aided RoFSO system over Mdistribution has been analyzed, and in this study, the Heteerodyne detection method was used. Closed-form expressions for PDF and CDF have been derived. The M-Quadrature Amplitude Modulation (QAM) in its binary form has been investigated, with emphasis on performance analysis through closed-form analytical expressions. System performance has been assessed using Outage Probability (OP) and Average Bit Error Rate (ABER) metrics, expressed analytically via the Meijer-G function. Different orders of QAM modulation schemes were comparatively analyzed in terms of their Average Bit Error Rate (ABER) performance It is shown that with RIS, RoFSO communication is possible without LOS. The proposed system can be applied to a smart city environment. In future work, we recommend that scenarios in which the line-of-sight (LoS) component is significant should be examined, as well as configurations involving multiple reconfigurable intelligent surface (RIS) links

Acknowledgement

This study is grounded in my MTech research conducted at the Harare Institute of Technology. I wish to express my deepest gratitude to the faculty and staff of the Department of Electronic Engineering for their invaluable support throughout this journey. In particular, I extend my sincere appreciation to my supervisor, Eng. S. Magidi, whose guidance and encouragement were instrumental to the successful completion of this research.

References

1. Ndjiongue, A.R., et al., *Performance analysis of RIS-based nT-FSO link over GG turbulence with pointing errors.* arXiv preprint arXiv:2102.03654, 2021.
2. Aghajanzadeh, S.M. and M. Uysal, *Multi-hop coherent free-space optical communications over atmospheric turbulence channels.* IEEE Transactions on Communications, 2011. **59**(6): p. 1657-1663.
3. Popoola, W.O., et al., *Free-space optical communication employing subcarrier modulation and spatial diversity in atmospheric turbulence channel.* IET optoelectronics, 2008. **2**(1): p. 16-23.
4. Moradi, H., H. Refai, and P. LoPresti, *Switch-and-stay and switch-and-examine dual diversity for high-speed free-space optics links.* IET optoelectronics, 2012. **6**(1): p. 34-42.
5. Cheng, M., et al., *Inverse Gaussian gamma distribution model for turbulence-induced fading in free-space optical communication.* Applied Optics, 2018. **57**(12): p. 3031-3037.
6. Jurado-Navas, A., et al., *A unifying statistical model for atmospheric optical scintillation.* Numerical simulations of physical and engineering processes, 2011. **181**(8): p. 181-205.
7. Tang, X., et al., *Multihop free-space optical communications over turbulence channels with pointing errors using heterodyne detection.* Journal of Lightwave Technology, 2014. **32**(15): p. 2597-2604.
8. Nistazakis, H., et al., *BER estimation for multi-hop RoFSO QAM or PSK OFDM communication systems over gamma gamma or*

exponentially modeled turbulence channels. Optics & Laser Technology, 2014. **64**: p. 106-112.

9. Dabiri, M.T., M.J. Saber, and S.M.S. Sadough. *BER performance of OFDM-based wireless services over radio-on-FSO links in the presence of turbulence and pointing errors*. in *2016 8th International Symposium on Telecommunications (IST)*. 2016. IEEE.
10. Kumar, A. and P. Krishnan, *RoFSO system based on BCH and RS coded BPSK OFDM for 5G applications in smart cities.* Optical and Quantum Electronics, 2022. **54**(1): p. 18.
11. El Saghir, B.M., M.B. El Mashade, and A.M. Aboshosha, *Performance analysis of MRR FSO communication system under Gamma–Gamma turbulence channel with pointing error.* Optics Communications, 2021. **489**: p. 126891.
12. Wang, Z., et al., *Performance comparison of different modulation formats over free-space optical (FSO) turbulence links with space diversity reception technique.* IEEE Photonics Journal, 2009. **1**(6): p. 277-285.
13. Petković, M. and G. Djordjević, *Average BER of dual-branch FSO system employing sim-bpsk influenced by Malaga atmospheric turbulence with pointing errors.* environment, 2017. **1**: p. 3.
14. Wang, H., et al., *Performance of wireless optical communication with reconfigurable intelligent surfaces and random obstacles.* arXiv preprint arXiv:2001.05715, 2020.
15. Yang, L., et al., *Free-space optical communication with reconfigurable intelligent surfaces.* arXiv preprint arXiv:2012.00547, 2020.
16. ElMossallamy, M.A., et al., *Reconfigurable intelligent surfaces for wireless communications: Principles, challenges, and opportunities.* IEEE Transactions on Cognitive Communications and Networking, 2020. **6**(3): p. 990-1002.
17. Atapattu, S., et al., *Reconfigurable intelligent surface assisted two–way communications: Performance analysis and optimization.* IEEE Transactions on Communications, 2020. **68**(10): p. 6552-6567.
18. Basar, E., *Reconfigurable intelligent surface-based index modulation: A new beyond MIMO paradigm for 6G.* IEEE Transactions on Communications, 2020. **68**(5): p. 3187-3196.
19. Wu, Q., et al., *Intelligent reflecting surface-aided wireless communications: A tutorial.* IEEE transactions on communications, 2021. **69**(5): p. 3313-3351.
20. Basar, E. and H.V. Poor, *Present and future of reconfigurable intelligent surface-empowered communications [perspectives].* IEEE Signal Processing Magazine, 2021. **38**(6): p. 146-152.
21. Ndjiongue, A.R., et al., *Design of a power amplifying-RIS for free-space optical communication systems.* IEEE Wireless Communications, 2022. **28**(6): p. 152-159.
22. Kumar, A. and P. Krishnan, *Performance analysis of RoFSO links with spatial diversity over combined channel model for 5G in smart city applications.* Optics Communications, 2020. **466**: p. 125600.
23. Kumar, A., P. Krishnan, and A.A.B. Raj, *Performance analysis of a RIS-assisted RoFSO communication system over Malaga distribution for smart city applications.* Applied Optics, 2023. **62**(19): p. 5325-5333.
24. Zhang, H. and B. Di, *Intelligent omni-surfaces: Simultaneous refraction and reflection for full-dimensional wireless communications.* IEEE Communications Surveys & Tutorials, 2022. **24**(4): p. 1997-2028.
25. Jurado-Navas, A., et al., *General analytical expressions for the bit error rate of atmospheric optical communication systems.* Optics letters, 2011. **36**(20): p. 4095-4097.
26. Ansari, I.S., F. Yilmaz, and M.-S. Alouini, *Performance analysis of free-space optical links over málaga ($\mathcal {M} $) turbulence channels with pointing errors.* IEEE Transactions on Wireless Communications, 2015. **15**(1): p. 91-102.
27. Wang, P., et al., *On the performances of relay-aided FSO system over M distribution with pointing errors in presence of various weather conditions.* Optics Communications, 2016. **367**: p. 59-67.
28. Yigit, Z., E. Basar, and I. Altunbas, *Low complexity adaptation for reconfigurable intelligent surface-based MIMO systems*. IEEE Communications Letters, 2020. **24**(12): p. 2946-2950.
29. Yang, L., et al., *On the performance of RIS-assisted dual-hop UAV communication systems.* IEEE Transactions on Vehicular Technology, 2020. **69**(9): p. 10385-10390.
30. Karp, D. and E. Prilepkina, *Hypergeometric differential equation and new identities for the coefficients of Nørlund and Bühring.* SIGMA. Symmetry, Integrability and Geometry: Methods and Applications, 2016. **12**: p. 052.
31. Adamchik, V.S. and O. Marichev. *The algorithm for calculating integrals of hypergeometric type functions and its realization in REDUCE system*. in *Proceedings of the international symposium on Symbolic and algebraic computation*. 1990.
32. Singh, H. and A.S. Sappal, *Analytic and simulative comparison of turbulent FSO system with different modulation techniques.* Optics & Laser Technology, 2019. **114**: p. 49-59.